Sensitive Device for Probing and Recognition of Obstacles in a Natural Environment

Lama Al Bassit, Hawraa Becher, Bastien Laurent, Hubert Villeneuve, Guillaume Jeanneau

Sensitive Device for Probing and Recognition of Obstacles in a Natural Environment

Hawraa BECHER, Lama Al-BASSIT*, Bastien LAURENT, Hubert VILLENEUVE, Guillaume JEANNEAU

Université Clermont Auvergne, INRAE, UR TSCF, 9 avenue Blaise Pascal CS 20085, F-63178 Aubière, France

*Corresponding author. Email: lama.al-bassit@inrae.fr

Abstract

Perception technologies used by mobile robots, based on cameras, LiDAR or RADAR can detect obstacles in the robot's path during navigation. However, the challenge lies in accurately differentiating between traversable and non-traversable obstacles. LiDAR alone can detect soft vegetation, like tall grass, and identify it as a non-traversable obstacle even though it might not affect neither the vehicle's movement nor safety. This paper introduces a mechanical device called a "Sensitive Bumper Probing System," which can be integrated into mobile robots and interact with the environment to help differentiating physically traversable from non-traversable obstacles and ensure the system's safe operation. To achieve this goal, the sensitive bumper provides force measurements as it interacts with the environment. Combined with a 2D LiDAR, this measurement permits to decide whether the detected obstacles are traversable and collects data about objects to contribute to the environment recognition.

Keywords: Robot-Obstacle Interaction, Traversability, Obstacle Probing, Perception by Direct Interaction, Sensitive Bumper, LiDAR.

1. Introduction

An autonomous vehicle operating in natural environment needs to be equipped with sensors to detect obstacles along its path. This is essential to avoid harmful collisions. Other than preserving the integrity of the vehicle, this also protects humans, animals, and other objects of the environment. For mobile robots, terrain traversability analysis is a critical task that directly affects the robot's performance and safety (Papadakis, 2013).

Research on terrain traversability can be divided into two main categories. The first is research on robot geometry and kinematics design to give a robot the ability to overcome obstacles without relying on perception. It is the case of the robot proposed by (Chavdarov et al., 2020) which has a specific wheel-leg geometry allowing it to advance and overcome obstacles. Alternatively, robots with specialized wheels are designed for better obstacle climbing ability. (Lee et al., 2020) propose a climbing robot whose wheels have inclined spokes. In addition to the omnidirectional deformable six-wheeled robot of (Huang et al., 2022), the Quadruped of (Chen et al., 2014), and the TurboQuad robot of (Chen et al., 2017) are examples of robots designed to overcome obstacles.

The other category is research on perception and sensory data processing for measuring terrain traversability. (Papadakis, 2013) distinguishes between two types of sensory data processing employed in this domain upon the need for physical contact: exteroceptive sensory data processing and proprioceptive sensory data processing.

Exteroceptive sensing methods analyze vision sensory data such as camera or LiDAR. They are common approaches for detecting obstacles and inferring their properties. As examples, (Lucas et al., 2019) propose a method for detecting linear vegetation elements in agricultural landscapes based on classification and segmentation of high-resolution LiDAR point data. (Ahtiainen et al., 2017) propose traversability mapping in outdoor environments based on LiDAR data. Similarly, (Broome et al., 2020) attempt to predict terrain traversability by using point clouds collected from laser rangefinders. Researchers from Southampton (Tomsett and Leyland, 2021) use an UAV equipped

with LiDAR and a multi-spectral camera to identify vegetation areas. (Takagaki et al., 2013) propose an image processing method to discriminate between traversable and non-traversable regions. (Kahn et al., 2021) develop a model that learns from a robot's experiences to navigate in outdoor environments, using RGB images and associated labels to identify tall grass as traversable. (Howard and Seraji, 2001) employ a technique that utilizes visual perception and a neural network to characterize and estimate terrain traversability. (Cunningham et al., 2015) propose a method for predicting the looseness of terrain by estimating its thermal inertia from temperature observations over a day. (Jiang et al., 2022) describe a solution using faster R-CNN for thermal images to detect pear tree trunks, enabling navigation under various lighting conditions in orchards.

Proprioceptive sensing is employed during the traversal of terrain. It is based on data issued from physical interaction between the robot and the environment using different types of sensors. In legged robots, for example, different sensing modalities are used to probe the ground and determine the robot-ground contact information. These sensing modalities include electric capacitance (Wu et al. 2016, 2020), pressure (Tenzer et al., 2014), airflow (Navarro et al., 2019), and magnetic Hall effect (Tomo et al., 2016) to detect varying forces. In (Haddeler et al., 2022) vision and terrain probing with force sensor are combined to analyze traversability. On autonomous ground vehicles (AGV), flexible contact bumpers are often used to detect impacts (Norcross et al., 2015). In (Armbrust et al., 2011), a highly responsive bumper system is developed to enable the RAVON robot to distinguish between passable vegetation and rigid obstacles. Bio-inspired whisker sensors using various approaches such as piezoresistive materials, optical fibers, or MEMS are also proposed to enhance robots' ability to interact with their environment and perform tasks like object detection, localization, and navigation (Yu et al., 2022).

In this project, the implementation of mechanical sensing system at the front of a mobile robot coupled to a LiDAR is investigated to analyze the traversability of the robot path. This paper proposes a new system called "Sensitive Bumper Probing System" (SBPS). It is composed of a 2D LiDAR and a mechanical device able to probe objects on the robot's path. SBPS allows differentiating between traversable obstacles (such as tall grass, foliage, etc.) and non-traversable obstacles. The concept of the sensitive bumper probing system is introduced in the following section (section 2) where the proposed design of the mechanical device and the operation principle of the system are described. Section 3 details the tests carried out to validate the concept of the sensitive bumper and the obtained results. The limitation of the system are discussed.

2. Materials and Methods

Giving a mobile robot the ability to decide to continue or to stop its planned trajectory when an object is detected on its path is the aim of our project. When the detected object is traversable, like tall grass, foliage, small branches, etc. (Figure 1), the decision of the robot must be to overcome the object and pursue its planned trajectory. For non-traversable objects like human, animal, tree trunk, etc., the robot decision must be to stop or to adapt its trajectory in order to avoid the obstacle.

Our robot detects the presence of obstacle-object by LiDAR. It probes the detected object with the sensitive bumper and measures their resistance to the advancement of the robot. Depending on the value of the measured force, the robot decides to continue its trajectory or to stop immediately. The following subsections introduce the design of the SBPS probing device and its operation principle.

a)  b) 

Figure 1. Examples of traversable objects, a) branches, b) plant

2.1. Sensitive Bumper concept

The proposed probing device is a sensitive bumper mounted on the front of the robot. It relies on the robot's progress to touch objects, probe them and measure their resistance to the advancement of the robot. To do so, before reaching the object, the robot's velocity slows down significantly (between 0.1 m/s to 0.2 m/s). Then, it continues its slow movement while the bumper is in contact with the object and until the measured effort passes a threshold.

The proposed sensitive bumper is composed of a moving assembly connected to the robot body by two parallel translational joints that each contains a spring and force sensor (Figure 2a).

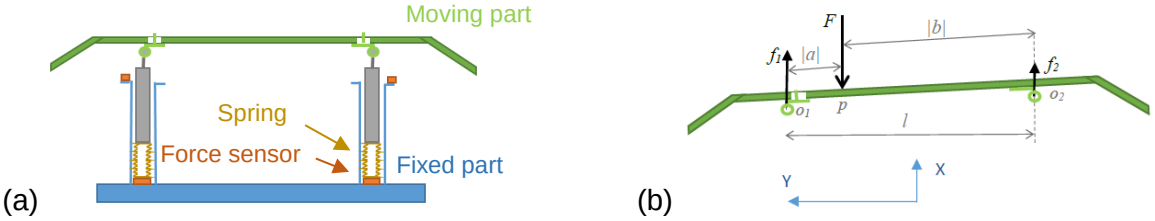

Figure 2. (a) Sensitive bumper concept and (b) force applied on the moving part, F, and measured forces f_1 and f_2

The sensitive bumper probing system is designed to measure the interaction force when in contact with an object. Wherever the contact point on the bumper is, the contact force, F, is obtained by adding the forces measured by the two force sensors, f_1 and f_2: $F=f_1+f_2$ (Figure 2b). The difference between the two force sensor measurements allows to determine the position of the contact point on the bumper.

A mathematical modelling of the bumper is established to study the influence of robot and bumper parameters on the forces applied on the probed objects. The case of probing rigid and fixed obstacle is considered. Before meeting the object, the robot moves at slow speed, V. When it meets the object, bumper springs, of stiffness k, are compressed and a force, F, is measured. When the value of the force reaches a threshold, F_l, the robot controlled speed drops to zero. During a response time, t_r, the robot continues its movement, then it decelerates and stops. The final force, measured when the robot stops, is then bigger than the threshold. For a safe probing, this final force must be minimized.

The theoretical study showed that, on the robot side, robot velocity when probing, V, and its response time, t_r, are the most influencing parameters on the final force. Other parameters like deceleration value and force threshold also influence the obtained final force. Figure 3(a) compare the forces obtained with two different velocities of probing (0.1 m/s and 0.2 m/s) while all the other parameters are fixed (t_r=0.1 s, F_l= 49 N, deceleration= 1.5 m/s2, k=3.6 N/mm). The force increases when the velocity increases. Figure 3(b) compares between forces obtained by a robot having a response time of 0.1s and another having a response time of 0.2 s. For the same impact velocity (0.2 m/s) and the same deceleration (1.5 m/s2), force threshold (49 N) and springs stiffness (3.6 N:mm), the robot having the higher response delay measures the highest forces.

On the bumper side, the spring's stiffness has the most significant influence on the measured force. The mass of the mobile assembly of the bumper has a limited influence in our case. Figure 3(c) shows plots of forces obtained when the springs stiffness is 3.6 N/mm then when it is 1.5 N/mm with the same probing conditions (V=0.2 m/s, t_r=0.1 s, F_l= 49 N, deceleration= 1.5 m/s2). The maximum value of force is obtained for the stiffer spring.

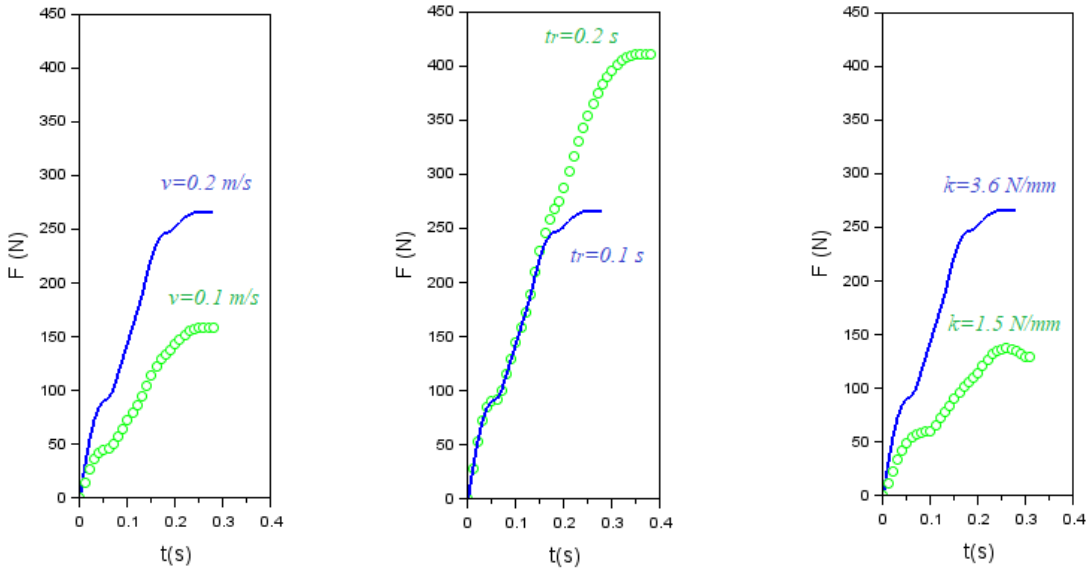

Figure 3. Force as function of time when probing a rigid and fixed object compared, a) for two different robot speeds (0.1 m/s and 0.2m/s), b) for two response times of the robot (0.1s and 0.2s) and c) for two bumper spring stiffness (3.6 N/mm and 1.5 N/mm)

The modeling of the sensitive bumper helps to adapt the new design on mobile robots. Two prototypes are built for tests, the first for a small robot with spring's stiffness of 3.6 N/mm and the other for a larger robot with spring stiffness of 1.5 N/mm. The corresponding propping speeds for these robots are respectively 0.1 m/s and 0.2 m/s. The approach to use the sensitive bumper is introduced in the next subsection.

2.2. System operation

The mobile robot, equipped with SBPS, detects the obstacle's presence in advance using the LiDAR. Then, if it is a known non-traversable obstacle, the robot will go around the obstacle and follow the trajectory. In the case of an unknown type of obstacle, the robot will reduce its speed and move towards it to measure the interaction force when contact happens. A measurement above a high threshold ensures a total stop of the robot.

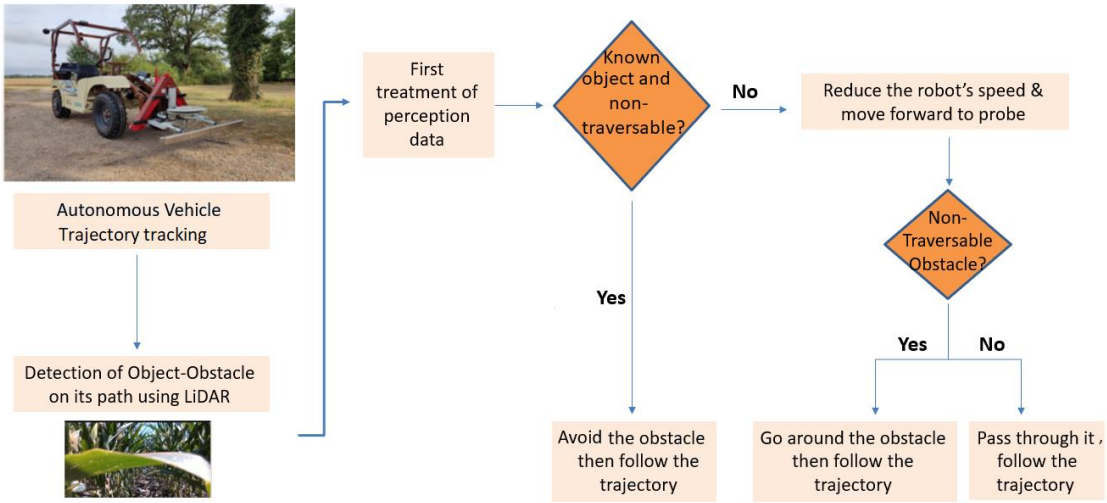

Figure 4. Flowchart of SBPS

System operation, as shown in Figure 4, needs to add the following functions to the robot:

- deciding if an object is a known non-traversable object based on a first perception from LiDAR data treatment;

- determining whether to traverse a probed object or to avoid it based on probing force data;
- adapting the robot's velocity with the situation;
- managing changes in the trajectory to go around a non-traversable object (not in the scope of this paper).

A first classification of obstacles detected remotely is executed using point clouds obtained from a 2D LiDAR. Initial observations showed that vegetation exhibits scattered points while some obstacles, especially walls, are characterized by aligned points. Scattered points can be grouped in clusters using RANSAC algorithm (Fischler and Bolles, 1981). For each cluster, its classification is done with respect to the regression line obtained through RANSAC. If the average distance of each point in the cluster to the regression line, or standard deviation (σ), is low, then the points are aligned on a straight line. In this case, the obstacle is considered to be a wall. A high standard deviation indicates scattered points, or vegetation (Figure 5).

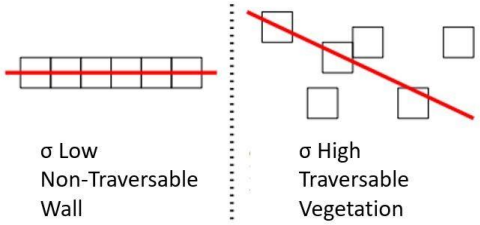

Figure 5. First approach of classification

The approach using LiDAR combined with the SBPS probing can enable distinguishing between traversable and non-traversable objects. Thus, the robot's velocity depends on the situation based on LiDAR and SBPS data. The velocity command can be summarized as shown in Table 1.

	Robot speed	*LiDAR data*		
		No nearby points detected	potentially traversable points	Non-traversable points
Bumper data	F < low threshold	Unchanged	Reduced	Null
	low threshold <F <high threshold	Reduced	Reduced	Null
	F > High threshold	Null	Null	Null

Table 1. Summary of velocity control laws

3. Results and Discussion

3.1. Probe concept validation tests

The new designed sensitive bumper probing system is mounted on "Effibote3 Robot", which weighs about 20 kg, with a Tim Sick LiDAR sensor (Figure 6). An Arduino microcontroller is used with a serial port to collect measurement data.

Figure 6. Sensitive bumper probing system mounted on "Effibote3 Robot"

Probing tests are carried out to validate the concept of the sensitive bumper and to assess the influence of different parameters on the forces measured by the bumper. A typical test goes through the following steps. (1) The robot follows a straight-line trajectory at 0.2 m/s faced to the object. (2) The robot slows to 0.1 m/s when under 2 m of distance to the tested object. (3) When the force sensors measure a contact force of 5 kg-force (49N), the robot speed drops to 0. The robot continues its

progress at 0.1 m/s in case the contact force is still lower than 5 kg-force. The tests that were conducted are listed as follow:

- Probing a tree trunk(Figure 7a).
- Probing a rigid wall at speeds of 0.1 m/s and 0.2 m/s while on smooth ground.
- Probing an 8 kg drum (Figure 7b), which can be filled with water up to 14 kg total, on smooth ground. This drum can be covered with foam for an additional external flexibility. The drum respects the test object dimensions given in ISO 18497:2018 intended to represent a small human. The test with 14 kg has the objective of validating whether or not the robot stops when the bumper probes a child having this mass.
- Probing tall grass.
- Rolling on different types of ground (grass, tall grass, bare soil and bitumen) at 0.1m/s and at 1m/s to study the influence of vibrations on the SBPS (Figure 7c).

(a) (b) (c)

Figure 7. Sample pictures of the SBPS validation tests, a) tree trunk, b) 8 kg drum and c) tall grass

Probing tests, carried out with SBPS, study the forces measured when probing different objects of the environment. The measured force when probing rigid and fixed objects shows, as depicted in Figure 8, that when the measured force, on the blue curve, reaches 5 kg-force the commanded speed of the robot, on the orange curve, decreases to zero. However, the measured force continues to rise up (to approximately 25 kg-force in the case of a wall probed at 0.2 m/s). This increase is due to response and braking time as shown in the theoretical study. The other tests produced at a lower speed of collision shows that the maximum value of the measured force decreases when the speed decreases.

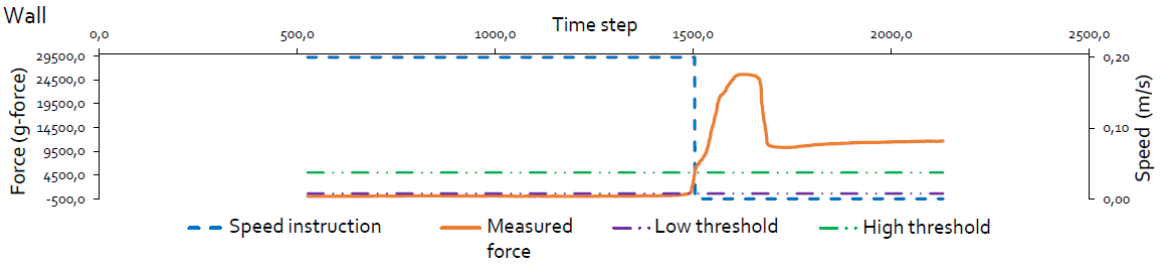

Figure 8. Measured forces and commanded speed while probing a rigid wall at 0.2 m/s with high threshold of 5 kg -force

Figure 9 represents the interaction between the robot and a drum on smooth ground (Figure 7b). This drum is filled with water to weigh 14 kg in total. The mass of the obstacle affects the maximum effort applied almost proportionally. Moreover, observations in these two cases (8 kg drum and14 kg drum) reveal that the initial collision did not surpass the upper threshold of 5 kg-force, causing the robot to slow down rather than stop. The force peak in the middle of the plot reflects the robot pushing the drum short distances before stopping, in the case of the 14 kg obstacle. To prevent pushing the obstacle, the threshold was lowered to 3 kg-force.

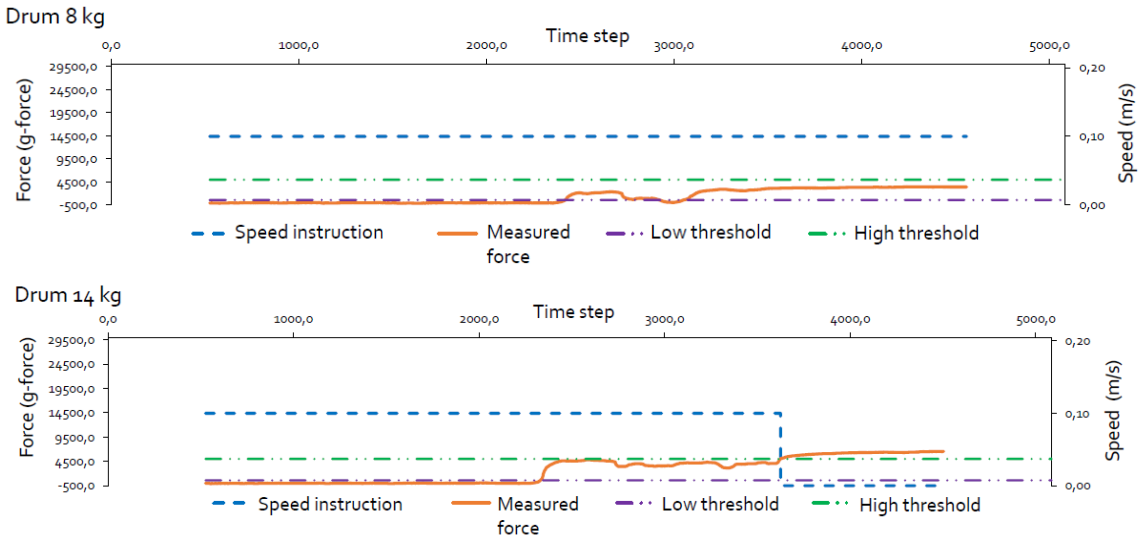

Figure 9. Measured forces and commanded speed while probing 8 kg object (top) and 14 kg object (down) with high threshold of 5 kg-force

The curves shown in Figure 10 depicts the most relevant scenario for the robots equipped with the SBPS. Indeed, one of this project's objectives is to navigate through tall grass even when the LiDAR detects an obstacle. Here, the maximum force reached is only 228 g-force. This is much lower and easily distinguishable from the case where the robot collides with an obstacle. Navigating through tall grass poses no significant challenge as long as the robot maintains a minimum speed, ensuring its integrity and the safety of its environment in the event of an unexpected collision.

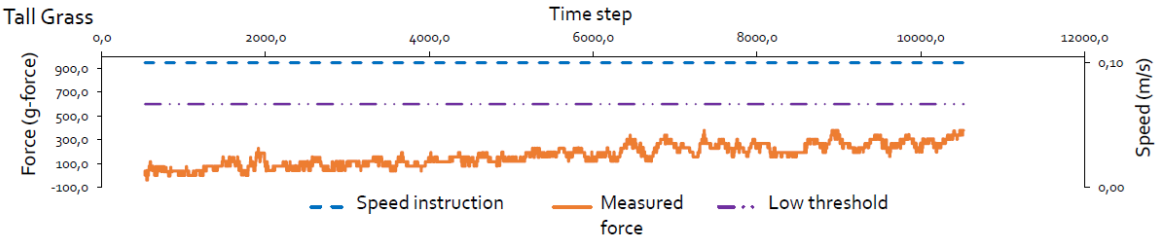

Figure 10. Measured forces and commanded speed while navigating through tall grass

Sensitive bumper tests and their results show the possibility to rely on force data to distinguish between traversable objects and non-traversable obstacles. A first level of classification (considering that the speed at probing is always less than 0.2 m/s) can be summarized as follows:

- Non-traversable obstacle when the measured force is greater than 3 kg-force
- Grass or other traversable vegetation when the measured force is less than 0.5 kg-force
- Ambiguous obstacles (such as an empty cardboard box) when the measured force is between 0.5 and 3 kg-force.

3.2. System operation testing

A numerical model was developed to test the system operation algorithms implemented for the different scenarios of SBPS. Gazebo simulation software allows us to observe the robot's navigation within the simulation environment. To be able to simulate the bumper under Gazebo and ROS middleware, an equivalent open-loop model of the bumper is used. This model is composed of one translational joint and one rotational joint (Figure 11). A linear and torsion springs are added to the joints to obtain a stiffness equivalent to that of the bumper. Contact bar displacements are measured through two laser range finders positioned at the location of the two translational joints of the real SPBS. The displacements are used to obtain the contact forces.

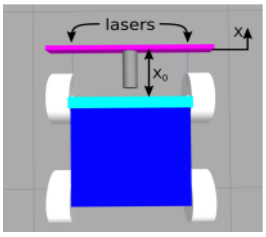

Figure 11. Numerical model of the sensitive bumper equipped to a mobile robot

The implemented algorithms allow the robot equipped with SBPS to take decisions related to traversability of the probed objects. Probing is not necessary if the robot detects a non-traversable obstacle, such as a wall, in advance. All other object geometries are considered potentially traversable and need to be probed to confirm their traversability. The steps of this first LiDAR data treatment are illustrated in Figure 12(a), using point cloud data visualized in Gazebo and RVIZ: a) shows a small robot with LiDAR surrounded by obstacles, including walls and rows of vegetation, in Gazebo. b) shows LiDAR data in RVIZ. In c) PointCloud voxelization, showing fewer points than in b). In d) clustering is carried out, and random color scales differentiate the groups. In e) the clusters are classified, distinguishing vegetation from walls. In f) only the points situated at a certain distance in front of the robot are retained.

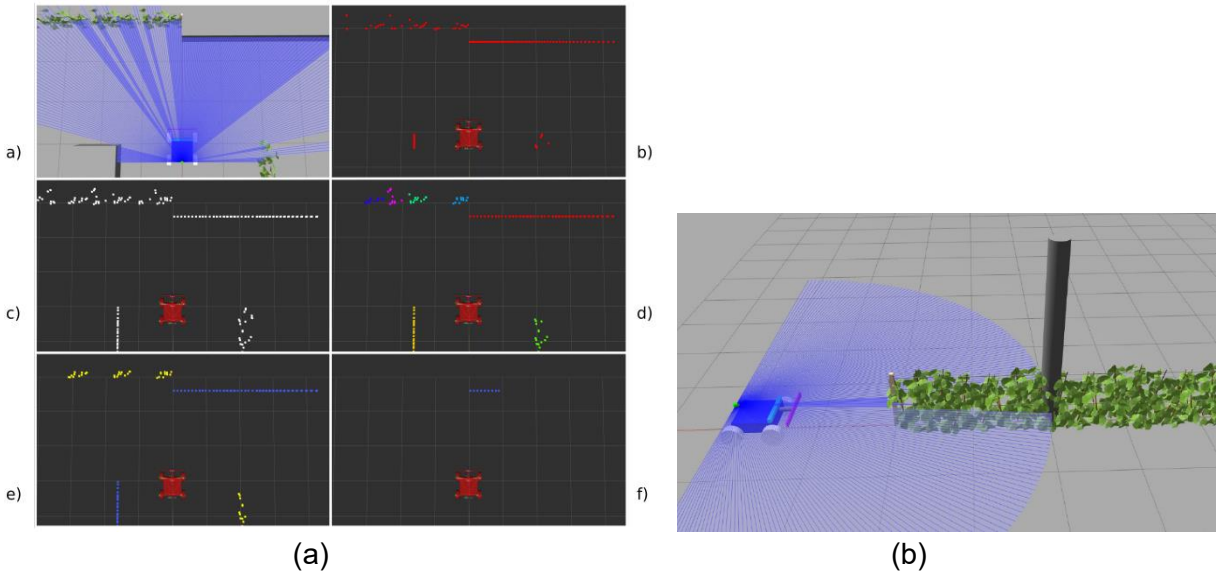

Figure 12. (a) Point cloud processing seen under Gazebo and RVIZ, (b) View of a simulated test

Different tests (simulated and real tests) are performed to validate the ability of the robot to decide and adapt its speed with respect to the encountered situation. In the simulated situation of Figure 12(b), the small robot slowed down its speed before reaching the plants, then it rolled through them at low speed and stopped when touching the fixed post.

3.3. System limitations

The SBPS produces interesting data that, combined with other perception data, can help in object classification and recognition. Even though, the proposed system has some limitations. Implementing and operating the sensitive bumper on a mobile robot requires that the robot has the ability to navigate at a very low speed (less than 0.2 m/s of controlled speed) in order to probe obstacles safely and that it has a short reaction and braking time to avoid applying significant forces on the environment.

Sensitive bumper with softer springs and greater maximum deformation reduces the forces applied during braking time. However, the design proposed for the sensitive bumper introduces friction in translational joints and does not help to increase displacements much. Regarding the geometry of the probing system, it could be interesting to probe objects at different heights. The presented geometry leads to a single direction and height probing.

Classifying obstacles as traversable, vegetation, or non-traversable, walls, done using LiDAR was shown, in Figure 12, to work well in a controlled environment. In a natural environment (Figure 13), however, the method is not as reliable. Figure 13(b) shows LiDAR data in RVIZ, taken in a tall grass field (green=traversable obstacles, black= non-traversable obstacles and red=non-identified obstacles). Some clusters on the left, highlighted in black, are incorrectly identified as walls due to being aligned on a straight line. In this case, the classification algorithm could be improved by either adapting the employed parameters or by changing the method altogether.

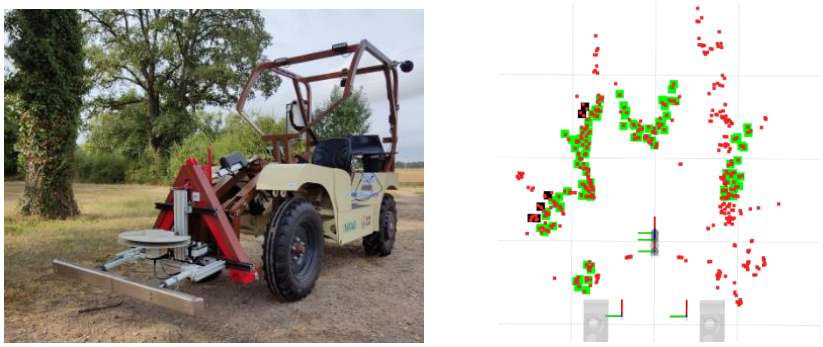

(a) (b)

Figure 13. (a) ALPO tractor robot equipped with SBPS and LMS Sick LiDAR, (b) Classification using LiDAR in tall grass field (green=traversable obstacles, black= non-traversable obstacles and red=non-identified obstacles)

Concerning the operation limitations, since the system is mainly used in agricultural environments with plenty of vegetation, such as tall grass or plants, the robot might always navigate with the minimum commanded speed, even if there is no necessity to probe objects.

4. Conclusions

The perception technologies used during the navigation of mobile robots, such as LiDAR, RADAR or camera, need complex algorithms or models to differentiate traversable from non-traversable obstacles. This paper discusses the design, implementation, and simulation of the “Sensitive Bumper Probing System.” The conducted probing tests make it possible to differentiate physically traversable from non-traversable obstacles. On the other hand, they ensure the safe operation of the system, which stops the robot if an object weighing more than 14 kg is probed. This device offers data, combined with other perception data, improving environmental recognition.

To simplify the operation of the robot for probing and to gather more data about objects’ characteristics, such as color, reflectance behavior, temperature, etc., an improved version of the mechanical sensing system called the “Proximity Sensitive-Whisker” is in prototyping phase.

Acknowledgments

We acknowledge M. Clément Dufor for his contributions to this work. We acknowledge the support of the Agence Nationale de la Recherche of the French government through the program ‘‘Investissements d’Avenir’’ (16-IDEX-0001 CAP 20-25).

References

Ahtiainen, J., Stoyanov, T., and Saarinen, J., “Normal distributions transform traversability maps: Lidar-only approach for traversability mapping in outdoor environments: Normal distributions transform traversability maps.” Journal of Field Robotics, 34(3) :600–621,, May 2017. https://doi.org/10.1002/rob.21657

Armbrust, C., Braun, T., Föhst, T., Proetzsch, M., Renner, A., Schäfer, B., and Berns, K., “Ravon: The robust autonomous vehicle for off-road navigation.” In Using Robots in Hazardous Environments, pages 353–396. Elsevier, 2011. https://doi.org/10.1533/9780857090201.3.353

Broome, M., Gadd, M., Martini, D. D., and Newman, P., “On the road: Route proposal from radar self-supervised by fuzzy lidar traversability,” AI, 1(4) :558–585,, Dec. 2020. https://doi.org/10.3390/ai1040033

Chavdarov, I., Krastev,, A., Naydenov B., and Pavlova, G., “Analysis and experiments with a 3d printed walking robot to improve climbing obstacle,” International Journal of Advanced Robotic Systems, Aug. 2020; 17(3), doi:10.1177/1729881420925282

Chen, S.-C., Huang, K.-J., Chen, W.-H., Shen, S.-Y., Li, C.-H., and Lin, P.-C., “Quattroped: A leg–wheel transformable robot,” IEEE/ASME Transactions on Mechatronics, vol. 19, no. 2, Apr. 2014, doi: 10.1109/TMECH.2013.2253615

Chen, W.-H., Lin, H.-S., Lin, Y.-M., and Lin, P.-C., "TurboQuad: A Novel Leg–Wheel Transformable Robot with Smooth and Fast Behavioral Transitions," IEEE TRANSACTIONS ON ROBOTICS, vol. 33, no. 5, Oct. 2017. doi: 10.1109/TRO.2017.2696022

Cunningham, C., Nesnas, I., and Whittaker, W. L., “Terrain traversability prediction by imaging thermal transients,” IEEE International Conference on Robotics and Automation (ICRA), Jul. 2015. Doi: 10.1109/ICRA.2015.7139750

Fischler M. A. and Bolles R.C., “Random sample consensus : a paradigm for model fitting with applications to image analysis and automated cartography,” Communications of the ACM 24.6 (juin 1981), p. 381-395, doi : 10.1145/358669.358692

Haddeler, G., Chuah, M. Y. M., You, Y., Chan, J., Adiwahono, A. H., Yau, W. Y., and Chew, C. M., “Traversability analysis with vision and terrain probing for safe legged robot navigation,” Robotic Control Systems, a section of the journal Frontiers in Robotics and AI. AI 9:887910, Aug. 2022. https://doi.org/10.3389/frobt.2022.887910

Howard A. and Seraji, H., “Vision-based terrain characterization and traversability assessment,” Journal of Robotic Systems, 18(10) :577–587, 2001, no. 10, 2001. https://doi.org/10.1002/rob.1046

Huang, Y., Meng, R., Yu, J., Zhao, Z., and Zhang, X., “Practical obstacle-overcoming robot with a heterogeneous sensing system: Design and experiments. machines,” Machines 2022, 10, 289., Apr. 2022. https://doi.org/10.3390/machines10050289

Jiang, A., Noguchi, R., and Ahamed, T., “Tree trunk recognition in orchard autonomous operations under different light conditions using a thermal camera and faster r-cnn,” Sensors, 22, 2065, 2022. https://doi.org/10.3390/s22052065

Kahn, G., Abbeel, P., and Levine, S., “An autonomous self-supervised learning-based navigation system,” IEEE Robotics and Automation Letters, vol. 6, no. 2, 2021, doi: 10.1109/LRA.2021.3057023

Lee, Y., Yoon, D., Oh, J., Kim, H. S., and Seo, T., “Novel angled spoke-based mobile robot design for agile locomotion with obstacle-overcoming capability,” IEEE/ASME Transactions on Mechatronics, vol. 1, no. 4, Aug. 2020, doi:10.1109/TMECH.2020.2992302

Lucas, C., Bouten, W., Koma, Z., Kissling, W. D., and Seijmonsbergen, A. C., “Identification of linear vegetation elements in a rural landscape using lidar point clouds,” Remote Sens, 11, 292, 2019, doi:10.3390/rs11030292

Navarro, S. E., Goury, O., Zheng, G., Bieze, T. M., and Duriez, C. “Modeling novel soft mechanosensors based on air-flow measurements,” IEEE Robot. Autom. Lett. 4, 4338–4345., 2019. https://doi.org/10.1109/LRA.2019.2932604

Norcross, R. J., Bostelman, R. V. and Falco, J. A., “Automated guided vehicle bumper test method development,” Technical Report NIST IR 8029, National Institute of Standards and Technology, May 2015.

Papadakis, P., “Terrain traversability analysis methods for unmanned ground vehicles: A survey,” Engineering Applications of Artificial Intelligence, Volume 26, Issue 4, 2013, Pages 1373-1385. https://doi.org/10.1016/j.engappai.2013.01.006

Takagaki, A., Masuda, R., Iida, M., and Suguri, M., “Image processing for ridge/furrow discrimination for autonomous agricultural vehicles navigation,” 4th IFAC Conference on Modelling and Control in Agriculture, Horticulture and Post Harvest Industry, Aug. 2013. https://doi.org/10.3182/20130828-2-SF-3019.00045

Tenzer, Y., Jentoft, L. P., and Howe, R. D., “The feel of mems barometers: Inexpensive and easily customized tactile array sensors,” IEEE Robot. Autom. Mag. 21, 89–95., 2014. https://doi.org/10.1109/MRA.2014.2310152

Tomo, T.P., Somlor, S., Schmitz, A., Jamone, L., Huang, W., Kristanto, H., and Sugano, S., “Design and characterization of a three-axis hall effect-based soft skin sensor,” Sensors 16, 491., 2016. http://dx.doi.org/10.3390/s16040491

Tomsett, C. and Leyland, J., “Development and testing of a uav laser scanner and multispectral camera system for eco-geomorphic applications,” Sensors, 2021. https://doi.org/10.3390/s21227719

Wu, X. A., Huh, T. M., Mukherjee, R., and Cutkosky, M., “Integrated ground reaction force sensing and terrain classification for small legged robots,” IEEE Robot.Autom. Lett. 1, 1125–1132., 2016. https://doi.org/10.1109/LRA.2016.2524073

Wu, X. A., Huh, T. M., Sabin, A., Suresh, S. A., and Cutkosky, M. R., “Tactile sensing and terrain-based gait control for small legged robots,” IEEE Transactions on Robotics, vol. 36, no. 1, Feb. 2020. https://doi.org/10.1109/TRO.2019.2935336

Yu, Z., Guo, Y., Huang, Q., Fukuda, T., Su, J., Cao, C., and Shi, Q., “Bioinspired, multifunctional, active whisker sensors for tactile sensing of mobile robots,” IEEE Robotics and Automation Letters, vol. 7, no. 4, Oct. 2022, doi: 10.1109/LRA.2022.3191172